STM JOURNALS

Journal of
Polymer & Composites

ISSN: 2321-2810 (Online)
ISSN: 2321-8525 (Print)
Volume 11, Special Issue 7, 2023
DOI (Journal): 10.37591/JoPC

http://engineeringjournals.stmjournals.in/index.php/JoPC/index

Research JoPC

Dispersion Analysis of TE Modes in 1D Magnetized Ferrite Photonic Crystals for Tunable and Switchable Band Gap Filtering Device Applications under Transverse Magnetization Configuration

Rajiv[1], Yogesh Sharma[1,*], M.T. Beig[2]

Abstract

The article comprehensively explores the dispersion characteristics exhibited by TE modes within one-dimensional magnetized ferrite photonic crystals, particularly under the influence of transverse magnetization. We employed the rigorous transfer matrix method, a powerful tool for theoretical investigation, calculation, and behavior analysis of such intricate systems. Our research delves into the structural parameters that govern the behavior of these ferrite photonic crystals, explicitly focusing on the incident parallel wave vector (β) and the filling factor (f) while also considering the impact of an external magnetic field. This multifaceted analysis reveals intriguing insights into the behavior of electromagnetic waves within these unique crystal structures. One of the key findings of our study is the profound influence of the filling factor (f) and the incident wave vector (β) on the emergence and properties of photonic band gaps (PBGs). Notably, as we increased both the filling factor (f) and the incident wave vector (β) while keeping the length of the period constant, we observed a significant effect on the allowed and forbidden band gaps. These band gaps shifted towards the higher wavelength region, illustrating the dynamic nature of these crystals in response to varying parameters. When β is equal to or greater than 3, no band is allowed, and the entire band appears to become a gap. This intriguing behavior suggests the potential utility of these structures as tunable and switchable band gap filtering devices with promising applications in various fields. Our comprehensive study sheds light on the intricate dispersion characteristics of TE modes within magnetized ferrite photonic crystals, offering valuable insights into their behavior under transverse magnetization. This research contributes to the fundamental understanding of these materials and opens doors to innovative applications in photonics band gap research application.

***Author for Correspondence**
Yogesh Sharma

[1]Research Scholar, Department of Physics, Shree Guru Gobind Singh Tricentenary University, Gurugram, Haryana, India
[1*]Assistant Professor, Department of Physics, Shree Guru Gobind Singh Tricentenary University, Gurugram, Haryana, India
[2]Assistant Professor, Department of Physics, Shree Guru Gobind Singh Tricentenary University, Gurugram, Haryana, India

Received Date: August 21, 2023
Accepted Date: September 13, 2023
Published Date: September 25, 2023

Citation: Rajiv, Yogesh Sharma, M.T. Beig. Dispersion Analysis of TE Modes in 1D Magnetized Ferrite Photonic Crystals for Tunable and Switchable Band Gap Filtering Device Applications under Transverse Magnetization Configuration. Journal of Polymer & Composites. 2023; 11(Special Issue 7): S60–S68.

Keywords: Ferrite photonic crystal, Magnetic Field, Dispersion behaviour, Photonic Band Gaps

INTRODUCTION

A lot of research has been done on magneto-optical photonic crystals (MOPhCs) because of their peculiar magneto-optical properties. MOPhCs (Magneto-Optical Photonic Crystals) structures have demonstrated significant potential in various technical fields [1-2]. They have been applied in integrated devices, cavity-enhanced Faraday rotation [3,4], non-reciprocal super-prisms [5,6], ultra-compact isolators [7,8], highly-directive miniature antenna arrays, and non-reciprocal propagation [9,10]. This composite

© STM Journals 2023. All Rights Reserved

periodic structure's electromagnetic (EM) responses are externally adjustable, and the parameters of the EM wave dispersion are affected by the external field. These MOPhCs have a geometry of media, including periodic arrangements of metal, dielectric, semiconductor, and other layers. Ferrite-based photonic crystals, sometimes called ferrite photonic crystals (FPhCs), waveguides, and transmission lines, are a current widespread issue in photonic research because of their unique properties.

In the study conducted by Z. Yu et al. [11], one-dimensional (1-D) Magneto-Optical Photonic Crystals (MOPhCs) were utilized to showcase one-way total reflections. These structures incorporated ferrites as one of the constituent layers within their unit cells. Recently, a ferrite-based circulator with independent polarisation was disclosed [12], according to A. M. Grishin et al. [13], considerable Faraday rotation and acceptable transmittance from the visible to infrared have been optimised for garnet-based MOPhCs. J.-X. Liu et al. [14] investigated the FPhCs' filtering capabilities.

The modelling and experimental validation of K. Bi et al.'s [15] work on the tunability of ferrite-dielectric metamaterials' dielectric properties. F. Fan et al. showed the existence of a magnetically tunable circulator in the terahertz frequency range [16]. V. I. Fesenko et al.'s [17] in-depth investigation of single-mode operation control in a spherical waveguide loaded with ferrites.

N. Dib et al. [18] employed magnetised ferrite material to mimic the propagation properties of cylindrical gearbox lines using the finite-difference time-domain approach and spectral-domain analysis. The dispersion characteristics of electromagnetic (EM) waves in magnetised 1-D FPhCs structures have recently been studied by Sharma and Prasad [19–20] for transverse electric (TE) and transverse magnetic (TM) modes in a variety of field settings, including longitudinal and transverse magnetization. The authors demonstrated that the EM waves' phase index and dispersion properties can be influenced by incident angle, filling factor, and external magnetic fields. These 1-D FPhCs structures exhibit dielectric properties in addition to magnetization. Ferrites in the sub-layer of a single cell of 1-D FPhCs structures are magnetised in these composite structures irrespective of the transverse or longitudinal orientations. It could be fascinating to look into such structures' EM wave dispersion properties.

THEORETICAL FORMULATIONS

Let's assume that the unit cell of a 1D magnetised FPhCs, as depicted in Figure 1, comprises alternating layers of YIG and NI ferrite material. We employed and with the staking period for the ferrite layer depth of YIG and NI, respectively. The EM wave moves in the x-z plane. The wave electric field in TE mode is orthogonal to the plane of propagation (pointing in the y-direction). The structure under study is predicted to be hit by an EM wave at an angle relative to the normal layer interface. Compared to the normstandarder interfaces, the incoming electromagnetic wave is at an angle. In the transverse magnetization setup, it is assumed that the externally supplied magnetic fields H_{01} and H_{02} are orthogonal to the plane of incidence.

After applying a magnetic field, the permeability of ferrite materials changes into a tensor quantity. A description of the transverse magnetization arrangement is given by Pozar et al. [21] for the permeability of ferrite materials:

$$\mu_f = \begin{pmatrix} \mu_r & 0 & j\mu_k \\ 0 & \mu_0 & 0 \\ -j\mu_k & 0 & \mu_r \end{pmatrix} \tag{1}$$

The components of ferrite permeability are as follows:

$$\mu_k = \frac{\omega_m \omega}{(\omega_0 - j\alpha\omega)^2 - \omega^2} \tag{2}$$

$$\mu_r = 1 + \frac{\omega_m(\omega_0 - j\alpha\omega)}{(\omega_0 - j\alpha\omega)^2 - \omega^2} \tag{3}$$

© STM Journals 2023. All Rights Reserved

Here ω_0 is the resonance frequency & the damping constant (α), a circular frequency (ω_m). The following are Maxwell time-dependent equations:

$$\nabla \times E = -\mu_0 \mu_f \frac{\partial H}{\partial t} \tag{4}$$

$$\nabla \times H = \varepsilon_0 \varepsilon_f \frac{\partial E}{\partial t} \tag{5}$$

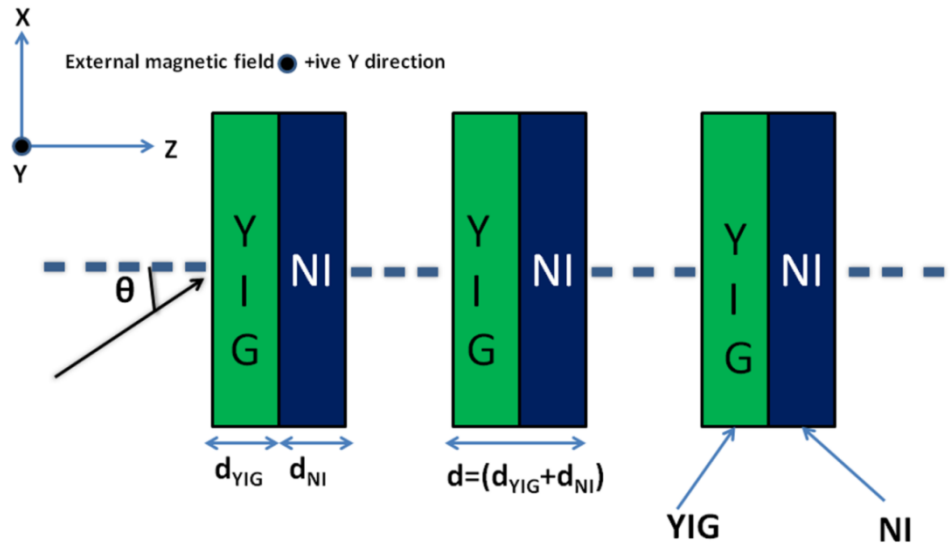

Figure 1. 1D magnetised FPhCs structure's unit cell schematic.

The magnetic and electric fields' constituent parts are listed as $E = (0, E_y, 0)e^{j\omega t}$ and $H = (H_x, 0, H_z)e^{j\omega t}$ in the TE mode. The Maxwell curl equations' electric and magnetic field components are stated as follows:

$$\frac{\partial E_y}{\partial z} = j\omega\mu_0[\mu_r H_x + j\mu_k H_z] \tag{6}$$

$$\frac{\partial E_y}{\partial x} = j\omega\mu_0[-\mu_r H_z + j\mu_k H_x] \tag{7}$$

$$\frac{\partial H_z}{\partial x} - \frac{\partial H_x}{\partial z} = -j\omega\varepsilon_0\varepsilon_f E_y \tag{8}$$

Eliminating the variables H_x & H_z from (2.6 & 2.7), we can find E_y satisfies the equation as mentioned below.

$$\frac{\partial^2 E_y}{\partial x^2} + \frac{\partial^2 E_y}{\partial z^2} = j\omega\mu_0 \left[\mu_r \left[\frac{\partial H_x}{\partial z} - \frac{\partial H_z}{\partial z}\right] + j\mu_k \left[\frac{\partial H_z}{\partial z} - \frac{\partial H_x}{\partial x}\right]\right] \tag{9}$$

$$\frac{\partial^2 E_y}{\partial x \partial z} = j\omega\mu_0 \left[\mu_r \frac{\partial H_x}{\partial x} + j\mu_k \frac{\partial H_z}{\partial x}\right] \tag{10}$$

$$\frac{\partial^2 E_y}{\partial z \partial x} = j\omega\mu_0 \left[-\mu_r \frac{\partial H_z}{\partial z} + j\mu_k \frac{\partial H_x}{\partial z}\right] \tag{11}$$

From, $\frac{\partial^2 E_y}{\partial x \partial z} = \frac{\partial^2 E_y}{\partial z \partial x}$

Using equations (2.9, 2.10 & 2.11), we have a final wave equation as:

© STM Journals 2023. All Rights Reserved

$$\frac{\partial^2 E_y}{\partial x^2} + \frac{\partial^2 E_y}{\partial z^2} + {k_1}^2 E_y = 0 \tag{12}$$

where $k_1 = (\omega/c)\sqrt{(\varepsilon_f/\mu_r) \times [({\mu_r}^2) + (j\mu_k)^2]}$ and ε_f is the ferrite layer's permittivity.

The YIG and NI ferrites layers make up the two sub-layers that make up each unit cell of 1D magnetised FPhCs. The solutions to wave equation (2.11) at interface I of the sublayer containing YIG are as follows:

$$E_y = (E_+ e^{-jk_{YIGz}} + E_- e^{jk_{YIGz}}) \times e^{j(\omega t - k_{YIGx} x)} \tag{13}$$

$$H_x = (A_{xf}^+ E_+ e^{-jk_{YIGz}} + A_{xf}^- E_- e^{jk_{YIGz}}) \times e^{j(\omega t - k_{YIGx} x)} \tag{14}$$

Here, $k_{YIGz} = (\omega/c) \times \sqrt{[({n_{fYIG}}^2) - (\beta)^2]}$ & $k_{YIGx} = (\omega/c) \times \beta$, $\beta = k_{YIGx}/(\omega/c)$

$$A_{xf}^+ = (1/\omega\mu_0) \times \left(-(\mu_{rYIG} k_{YIGz} + j\mu_{kYIG} k_{YIGx})\right)/\left(({\mu_{rYIG}}^2) + (j\mu_{kYIG})^2\right)$$

$A_{xf}^- = (1/\omega\mu_0) \times ((\mu_{rYIG} k_{YIGz} - j\mu_{kYIG} k_{YIGx}))/\left(({\mu_{rYIG}}^2) + (j\mu_{kYIG})^2\right)$ & $n_{fYIG} = \sqrt{(\varepsilon_{fYIG}/\mu_{rYIG}) \times [({\mu_{rYIG}}^2) + (j\mu_{kYIG})^2]}$.

The forward and backward amplitude (A_{xf}^+ & A_{xf}^-) moving waves in the YIG sub-layer are represented here by (A_{xf}^+ & A_{xf}^-). The equation (2.13) can be decomposed into tangential components of electric and magnetic fields at interface I:

$$E_y\big|_{at\ I\ interface} = E_I = (E_+ e^{-j(k_{YIGz} z)} + E_- e^{j(k_{YIGz} z)}) \times e^{j(\omega t - k_{YIGx} x)} \tag{15}$$

$E_{i_{1y}}$ $E_{r_{1y}}$

Similarly magnetic field (equation (2.15)) at interface I:

$$H_x\big|_{at\ I\ interface} = H_I = (A_{xf}^+ E_+ e^{-i(k_{YIGz} z)} + A_{xf}^- E_- e^{i(k_{YIGz} z)}) \times e^{j(\omega t - k_{YIGx} x)} \tag{16}$$

$H_{i_{1x}}$ $H_{r_{1y}}$

The incident reflected/transmitted components of the electric and magnetic fields can also be used to decompose the electric and magnetic field at boundary II.

The E & B fields interfaces I and II are described in terms of incident, reflected, and transmitted waves as follows:

$$E_I = E_{i_{1y}} + E_{r_{1y}} = E_{t_{1y}} + E_{r'_{2y}} \tag{17}$$

$$H_I = H_{i_{1x}} + H_{r_{1x}} = H_{t_{1x}} + H_{r'_{2x}} \tag{18}$$

$$E_{II} = E_{i_{2y}} + E_{r_{2y}} = E_{t_{2y}} + E_{r'_{3y}} \tag{19}$$

$$H_{II} = H_{i_{2x}} + H_{r_{2x}} = H_{t_{2x}} + H_{r'_{3x}} \tag{20}$$

At boundary I, we have the incident, reflected, and transmitted electric and magnetic fields denoted by $\left(E_{i_{1y}}, H_{i_{1x}}\right)$, $(E_{r_{1y}}, H_{r_{1x}})$, $(E_{t_{1y}}, H_{t_{1x}})$, $E_{r'_{2y}}$ and $H_{r'_{2x}}$, respectively. The electric and magnetic

© STM Journals 2023. All Rights Reserved

field components$E_{r'_{2y}}$ and $H_{r'_{2x}}$ represent the reflection of fields from boundary II to boundary I. At boundary II, we have the incident, reflected, and transmitted electric field components, $E_{i_{2y}}, E_{r_{2y}} \& E_{t_{2y}}$ as well as the incident, reflected, and transmitted magnetic field components$H_{i_{2x}}, H_{r_{2x}} and H_{t_{2x}}$. Furthermore, $E_{r'_{3y}}$ and $H_{r'_{3x}}$represent the reflection of the wave field from boundary III (not shown in Figure 2) to boundary II. To ensure the smooth transition between boundary I and boundary II, certain continuity conditions must be met by the electric and magnetic field components E_y and H_x, as presented below:

$$\begin{pmatrix} H_I \\ E_I \end{pmatrix} = \begin{pmatrix} A_{xf}^{+} & A_{xf}^{-} \\ 1 & 1 \end{pmatrix} \begin{pmatrix} E_{t_{1y}} \\ E_{r'_{2y}} \end{pmatrix} \tag{21}$$

$$\begin{pmatrix} H_{II} \\ E_{II} \end{pmatrix} = \begin{pmatrix} A_{xf}^{+} & A_{xf}^{-} \\ 1 & 1 \end{pmatrix} \begin{pmatrix} E_{i_{2y}} \\ E_{r_{2y}} \end{pmatrix} \tag{22}$$

$$\begin{pmatrix} E_{i_{2y}} \\ E_{r_{2y}} \end{pmatrix} = \begin{pmatrix} e^{-jk_{YIGz}d_{YIG}} & 0 \\ 0 & e^{jk_{YIGz}d_{YIG}} \end{pmatrix} \begin{pmatrix} \mathrm{E_{t_{1y}}} \\ E_{r'_{2y}} \end{pmatrix} \tag{23}$$

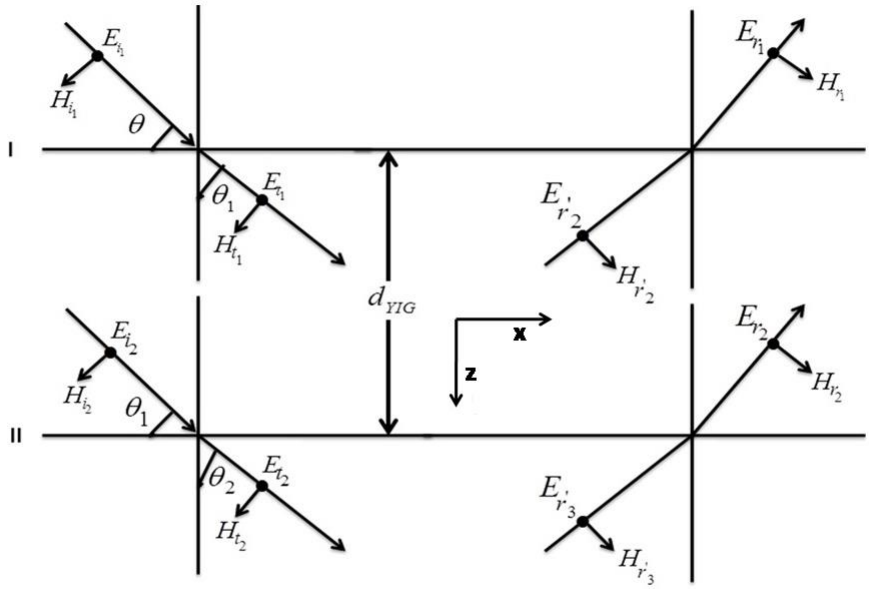

Figure 2. The YIG layer's sub-layer's wave electric and magnetic field components.

After calculation by using the above equations, we derived the following equation:

$$\begin{pmatrix} H_I \\ E_I \end{pmatrix} = M_1 \begin{pmatrix} H_{II} \\ E_{II} \end{pmatrix} \tag{24}$$

The elements of $M_1$for YIG layer are:

$$M_1 = \begin{pmatrix} \cos(k_{YIGz}d_{YIG}) - \left(\frac{(\mu_{k_{YIG}}k_{YIGx})}{(\mu_{r_{YIG}}k_{YIGz})}\right) \times sin(k_{YIGz}d_{YIG}) & -\frac{j}{\eta_1}\left(1 + \left(\frac{\mu_{k_{YIG}}k_{YIGx}}{\mu_{r_{YIG}}k_{YIGz}}\right)^2\right) \times sin(k_{YIGz}d_{YIG}) \\ -j\eta_1 \times sin(k_{YIGz}d_{YIG}) & \cos(k_{YIGz}d_{YIG}) - \left(\frac{(\mu_{k_{YIG}}k_{YIGx})}{(\mu_{r_{YIG}}k_{YIGz})}\right) \times sin(k_{YIGz}d_{YIG}) \end{pmatrix} \tag{25}$$

Similarly, for NI ferrite layer:

© STM Journals 2023. All Rights Reserved

$$M_2 = \begin{pmatrix} \cos(k_{NIz}d_{NI}) - \left(\frac{(\mu_{k_{NI}}k_{NIx})}{(\mu_{r_{NI}}k_{NIz})}\right) \times sin(k_{NIz}d_{NI}) & -\frac{j}{\eta_2}\left(1 + \left(\frac{\mu_{k_{NI}}k_{NIx}}{\mu_{r_{NI}}k_{NIz}}\right)^2\right) \times sin(k_{NIz}d_{NI}) \\ -j\eta_2 \times sin(k_{NIz}d_{NI}) & \cos(k_{NIz}d_{YIG}) - \left(\frac{(\mu_{k_{NI}}k_{NIx})}{(\mu_{r_{NI}}k_{NIz})}\right) \times sin(k_{NIz}d_{NI}) \end{pmatrix} \quad (26)$$

Here $k_{NI} = (\omega/c)\sqrt{(\varepsilon_{fNI}/\mu_{rNI}) \times [(\mu_{rNI}{}^2) + (j\mu_{kNI})^2]}$, $k_{NIz} = (\omega/c) \times \sqrt{[(n_{fNI}{}^2) - (\beta)^2]}$, $k_{NIx} = (\omega/c) \times \beta$, $\eta_1 = (\omega \times \mu_0) \times \sqrt{(\mu_{rYIG}{}^2 + (j \times \mu_{kYIG})^2)/(\mu_{rYIG} \times k_{YIGz})}$, $\eta_2 = (\omega \times \mu_0) \times \sqrt{(\mu_{rNI}{}^2 + (j \times \mu_{kNI})^2)/(\mu_{rNI} \times k_{NIz})}$ and $n_{fNI} = \sqrt{(\varepsilon_{fNI}/\mu_{rNI}) \times [(\mu_{rNI}{}^2) + (j\mu_{kNI})^2]}$. M=$M_1M_2$ is used to calculate the transfer matrix for the unit cell. M_{11}, M_{12}, M_{21}, and M_{22} are the last elements we obtain after multiplying M_1 and M_2. So,

$$\begin{pmatrix} H_I \\ E_I \end{pmatrix} = \begin{pmatrix} m_{11} & m_{12} \\ m_{21} & m_{22} \end{pmatrix} \begin{pmatrix} H_{II} \\ E_{II} \end{pmatrix} \quad (27)$$

Using the transfer matrix elements in equation (2.27) the dispersion relation for the 1-D magnetised FPhCs is provided as follows:

$$K = \left({}^1/_d\right) \times \cos^{-1}(0.5 \times (m_{11} + m_{12})) \quad (28)$$

where *K* is Bloch wave number.

RESULTS AND DISCUSSION

This article examined the effects of external magnetic fields, the filling factor and normalized parallel wave vector (β)on the band structure and phase index of the 1D magnetised FPhCs. We employed YIG (Yttrium iron garnet) layer and (Nickel Ferrite) NI layer thicknesses in this study as $a_{YIG} = f\lambda_0/4n_1$ and $b_{NI} = (2-f)\lambda_0/4n_2$. Here f is the filling factor, $\lambda_0 = (2\pi c/\omega_{mYIG}), \omega_{mYIG} = 2\pi f_{mYIG}, f_{mYIG} = (2.8 \times 10^6 \times M_{sYIG})$. Other important parameters studied are resonance frequency corresponding to YIG and NI ferrite layers. The evaluated values for external magnetic field (H_{01} & H_{02}) are tabulated in Table 1.

Table 1. External magnetic field values studied:

ω_{0YIG}	ω_{0NI}	Gyro-magnetic ratio γ
$2\pi f_{0YIG}$ $f_{0YIG} = (2.8 \times 10^6 \times H_{01})$	$2\pi f_{0NI}$ $f_{0NI} = (2.8 \times 10^6 \times H_{02})$	$2.8\ MHzOe$

The circular frequencyω_m $(= 2\pi\gamma M_s)$ with saturation magnetization M_s and normalized parallel incident wave vector, $\beta = k_{1x}/(\omega/c)$ (Table 2).

Table 2. Dielectric constants, Damping constants and saturation magnetization were studied:

Name	Dielectric constants (ε)	Damping constants (α)	Saturation magnetization (M_s)
YIG	15.0	2×10^{-4}	$M_{sYIG} = 1780\ Oe$
NI ferrites	9.0	8×10^{-4}	$M_{sNI} = 500\ Oe$

The resonance frequencies corresponding to the photonic crystals layer under study (YIG and NI) in transverse magnetization configuration [22] is computed. The expressions used are $\omega^2{}_{01} = \omega_{0YIG}(\omega_{0YIG} + \omega_{m_{YIG}})$ and $\omega^2{}_{02} = \omega_{0NI}(\omega_{0NI} + \omega_{m_{NI}})$ YIG and NI layer respectively. We consider

© STM Journals 2023. All Rights Reserved

the values of external magnetic fields (H01 = 46 Oe and H02 = 155 Oe) for YIG and NI ferrites here Oe represents Oersted. Pozar et al. [21] (2004) reported that the trans-tech numbers assigned to YIG ferrite and NI ferrite are G-113 and TT2-113, respectively. All computations maintain constant saturation magnetization, damping constants, and dielectric constant values.

Variation of frequency and (*β*) at filling factor (*f*)

If we increase the filling factor from f = 0.1, 0.5 & 1, keeping length of the period constant at the above of saturation magnetization for ferrite (YIG) = 46 Oe and ferrite Nickel (NI) = 155 Oe we observed that allowed and forbidden band gap appears and shift towards higher Wavelength region.

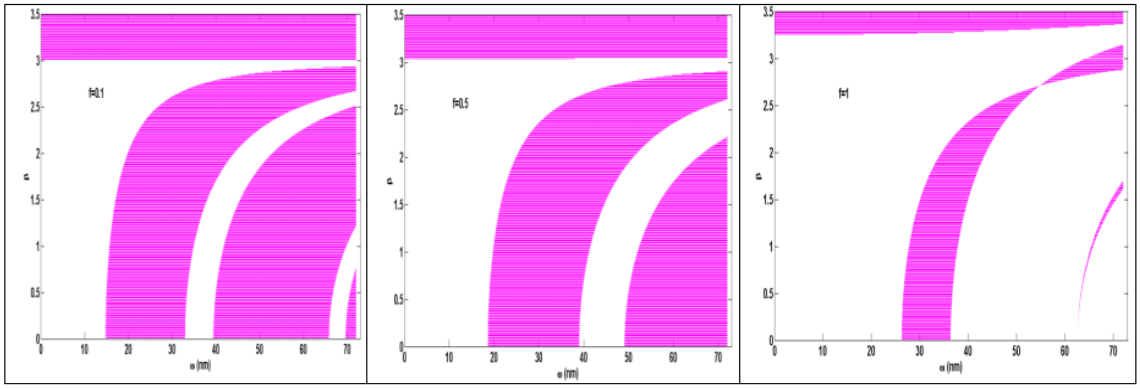

Fig. 3(a) Variation of frequency (nm) & β at f=0.1	Fig. 3(b) Variation of frequency (nm) & β at f=0.5	Fig. 3(c) Variation of frequency (nm) & β at f=1

At the value for β = 3 and above, no band is allowed and appears complete band gap. As shown below, Figs. 3(a), 3(b) & 3(c) at f=0.1, 0.5 & 1.

Analysis of Frequency and Filling Factor Variation

If we increase the incident angle β = 1.1, 1.5 & 2.5, at the above of saturation magnetization for ferrite YIG=46 Oe and ferrite NI=155 Oe then we observed that allowed and forbidden band gap appears and shift towards higher Wavelength region.

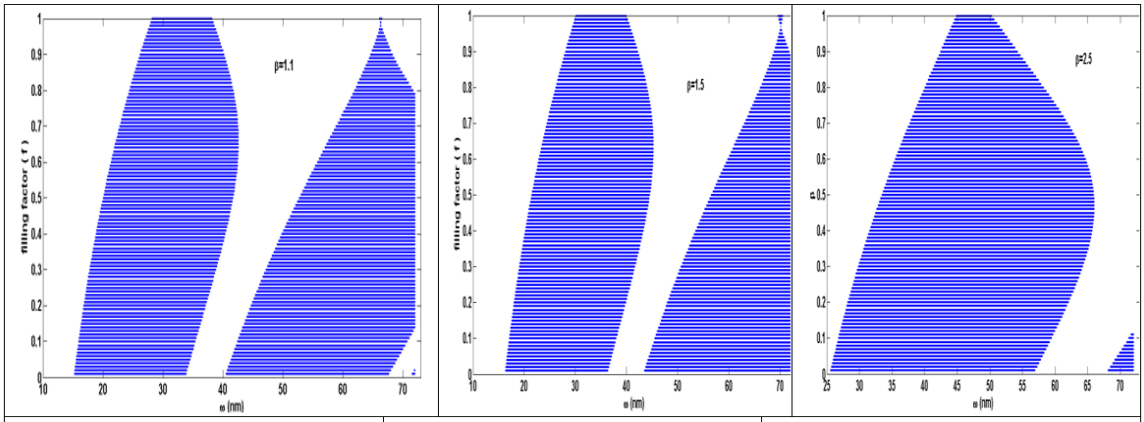

Fig. 4(a) Variation of ω with filling factor at β=1.1	Fig. 4(b) Variation of ω with filling factor at β=1.5	Fig. 4(c) Variation of ω with filling factor at β=1.1

At the value of β=3 and above, no band is allowed and appears completely band gap. As shown below, figs. 4(a), 4(b) & 4(c) at β = 1.1, 1.5 & 2.5.

CONCLUSIONS

© STM Journals 2023. All Rights Reserved

This research paper comprehensively explores the intriguing dispersion behaviour and phase index characteristics exhibited by magnetised 1D FPhCs. Employing a meticulous transfer matrix approach, we conduct a thorough analysis to unravel the intricate interplay of various factors, including the filling factor (f) and external magnetic fields, on the dispersion properties of these fascinating structures. We have examined the impact of different parameters on the dispersion properties of magnetised 1D FPhCs. Specifically, shedding light on the profound influence of the f and external magnetic fields on the behaviour of PBGs, regions in the electromagnetic spectrum where specific frequencies are forbidden from propagating within the crystal structure.

Our findings reveal a captivating relationship between the angular frequency (ω) and the incident parallel wave vector (β) at a consistent filling factor. We have uncovered that, as the value of β increases, the photonic band gaps exhibit a remarkable expansion in their width. This phenomenon underscores the intricate interplay between the incident wave vector and the propagation characteristics within the magnetised 1D FPhCs.Furthermore, we studied frequency variation concerning the f while keeping the incident wave vector β constant. Within this context, we make a fascinating observation – the photonic band gaps manifest as distinct lobes. These lobes, indicative of specific frequency ranges, provide valuable insights into the behaviour of light propagation within the intricate lattice structure of the FPhCs.

Notably, our investigations also unveil a compelling correlation between the order of PBGs and the number of lobes observed in the frequency variation with the filling factor. As the order of PBGs increases, a proportional rise in the number of lobes is evident. This intriguing relationship highlights the intricate and systematic dispersion behaviour within the magnetised 1D FPhCs.

Our research delves deeply into magnetised one-dimensional ferrite photonic crystals' dispersion characteristics and phase index behaviour. We meticulously analyse the effects of filling factor and external magnetic fields and uncover intricate relationships between angular frequency, incident wave vectors, and the emergence of photonic band gaps as lobes. Our findings contribute to a nuanced understanding of the behaviour of light within these unique crystal structures, opening avenues for further exploration and potential applications in photonics and electromagnetic wave manipulation.

Acknowledgments

The authors appreciate Prof. Vivek Singh and Prof. S. Prasad's support and encouragement. Corresponding Author Dr. Yogesh Sharma (Principal investigator) acknowledges the Science and Engineering Research Board Core Research Grant (SERB-CRG) Project No. CRG/2022/006820, New Delhi, for providing the financial support.

REFERENCES

1. Vasiliev M, Alameh K, Belotelov V, Kotov VA, and Zvezdin AK, “Magnetic photonic crystals: 1-D optimization and applications for the integrated optics devices,” J. Lightwave Technol., 2006.
2. Zamani M, and Ghanaatshoar M, “Miniaturized magnetophotonic crystals for multifunction applications in infrared region,” Opt. Eng., 2015, vol. 54(9), pp. 097103-1-097103-8.
3. Inoue M, Arai K, Fujii T, and Abe M, “Magneto-optical properties of one-dimensional photonic crystals composed of magnetic and dielectric layers,” J. Appl. Phys., 1998, vol. 83 (11), pp. 6768-6770.
4. Steel MJ, Levy M, and Osgood Jr. RM, “High transmission enhanced Faraday rotation in one-dimensional photonic crystals with defects,” IEEE. Photon. Technol. Lett., 2000, vol. 12, pp. 1171–1173.
5. Bita I, and Thomas EL, “Structurally chiral photonic crystals with magneto-optic activity: indirect photonic bandgaps, negative refraction, and super-prism effects,” J. Opt. Soc. Am. B, 2005, vol. 22(6), pp. 1199-1210.

© STM Journals 2023. All Rights Reserved

6. Wang Z, and Fan S, "Optical circulators in two-dimensional magneto-optical photonic crystals," Opt. Lett., 2005, vol. 30 (15), pp. 1989-1991.
7. Wolfe R, Lieberman RA, Fratello VJ, Scotti RE, and Kopylov N, "Etch-tuned ridged waveguide magneto-optic isolator," Appl. Phys. Lett., 1990, vol. 56, pp. 426-428.
8. Mumcu G, Sertel K, Volakis JL, Vitebskiy I, and Figotin A, "RF propagation in finite thickness nonreciprocal magnetic photonic crystals," IEEE APS Symposium 2004, Vol. 2, pp. 1395–1398.
9. Figotin A and Vitebsky I, "Electromagnetic unidirectionality in magnetic photonic crystals," Phys. Rev. B, 2003, vol. 67, pp. 165210-1- 165210-20.
10. Liu SY, Lu WL, Z. Lin F, Chui ST, "Magnetically controllable unidirectional electromagnetic wave guiding devices designed with metamaterials," Appl. Phys. Lett., 2010, vol. 97, pp. 201113-1- 201113-3.
11. Yu Z, and Wang Z, "One-way total reflection with one-dimensional magneto-optical photonic crystals," Appl. Phys. Lett., vol. 90, pp. 121133-1-121133-3, 2007.
12. Xi X, Lin M, Qiu W, Ouyang Z, Wang Q, and Liu Q, "Polarization-independent circulator based on ferrite and plasma materials in two-dimensional photonic crystal," Scientific Reports, 2018, vol. 8, pp. 1-12.
13. Grishin A.M, and Khartsev SI, "All-garnet magneto-optical photonic crystals," J. Magn. Soc. Jpn., vol. 32, pp. 140-145, 2008.
14. Liu JX, Xu HY, Yang ZK, Xie X, Zhang Y, and Yang HW, "A research of magnetic control ferrite photonic crystal filter," Plasmonics, 2017, vol. 12, pp. 971–976.
15. Bi K, Huang K, Zeng LY, Zhou MH, Wang QM, Wang YG, and Lei M, "Tunable dielectric properties of ferrite-dielectric based metamaterial," PLoS ONE., vol. 10, pp. 1-8, 2015.
16. Fan F, Chang SJ, Niu C, Hou Yu, Wang XH, "Magnetically tunable silicon-ferrite photonic crystals for terahertz circulator," Opt. Commun., vol. 285, pp. 3763-3769, 2012.
17. Fesenko VI, Tuz VR, Fedorin IV, Sun HBo, V. M. Shulga and Wei Han, "Control of single-mode operation in a circular waveguide filled by a longitudinally magnetized gyro electromagnetic medium," J. Electromag. Wave., 2017 vol. 31(13), pp. 1265-1276.
18. Dib N, and Omar A, "Dispersion analysis of multilayer cylindrical transmission lines containing magnetized ferrite substrates," IEEE Trans. Microw. Theory Tech., 2002, vol. 50, pp. 1730-1736.
19. Sharma Y, and Prasad S, "Dispersion properties of one-dimensional magnetized ferrite photonic crystals in transverse magnetization configuration for transverse magnetic modes," Eur. Phys. J. D, 2018, vol. 73, pp. 166-1-166-10.
20. Sharma Y, and Prasad S, "Properties of dispersion and phase index in magnetized one-dimensional ferrite photonic crystals in longitudinal configuration for TM mode," Superlattice Microst., vol. 120, pp. 463-472, 2018.
21. Pozar DM, Microwave Engineering, 3rd ed., Wiley publication New York, 2004.
22. Igarashi M, and Naito Y,"Tensor permeability of partially magnetized ferrites," IEEE. Transactions on Magnetics, 1977, vol. 13, pp. 1664–1668.

© STM Journals 2023. All Rights Reserved